THE JOURNAL OF BIOLOGICAL CHEMISTRY VOL. 289, NO. 4, pp. 1993–2001, January 24, 2014
Published in the U.S.A.

Multiple Roles of the $SO_4^{2-}/Cl^-/OH^-$ Exchanger Protein Slc26a2 in Chondrocyte Functions*

Received for publication, July 18, 2013, and in revised form, November 21, 2013 Published, JBC Papers in Press, December 3, 2013, DOI 10.1074/jbc.M113.503466

Meeyoung Park[‡], Ehud Ohana[§], Soo Young Choi[¶], Myeong-Sok Lee[‡], Jong Hoon Park[‡1], and Shmuel Muallem[§2]

From the [‡]Department of Biological Science, Research Center for Women's Disease, Sookmyung Women's University, Seoul 140-742, Republic of Korea, the [§]Epithelial Signaling and Transport Section, Molecular Physiology and Therapeutics Branch, National Institute of Dental and Craniofacial Research, National Institutes of Health, Bethesda Maryland 20892, and the [¶]Department of Biomedical Science and Research Institute of Bioscience and Biotechnology, Hallym University, Chuncheon 200-702, Republic of Korea

Background: Slc26a2 is a SO_4^{2-} transporter that is mutated in diastrophic dysplasia. The role of Slc26a2 in several chondrocyte functions is unknown.
Results: Slc26a2 is activated by IGF-1 to regulate chondrocyte, proliferation, differentiation, proteoglycan synthesis, and size.
Conclusion: Slc26a2 regulates multiple SO_4^{2-}-dependent and SO_4^{2-}-independent chondrocyte functions.
Significance: The findings should help in understanding aberrant SLC26A2 function in diastrophic dysplasia.

Mutations in the $SO_4^{2-}/Cl^-/OH^-$ exchanger Slc26a2 cause the disease diastrophic dysplasia (DTD), resulting in aberrant bone development and, therefore, skeletal deformities. DTD is commonly attributed to a lack of chondrocyte SO_4^{2-} uptake and proteoglycan sulfation. However, the skeletal phenotype of patients with DTD is typified by reduction in cartilage and osteoporosis of the long bones. Chondrocytes of patients with DTD are irregular in size and have a reduced capacity for proliferation and terminal differentiation. This raises the possibility of additional roles for Slc26a2 in chondrocyte function. Here, we examined the roles of Slc26a2 in chondrocyte biology using two distinct systems: mouse progenitor mesenchymal cells differentiated to chondrocytes and freshly isolated mouse articular chondrocytes differentiated into hypertrophic chondrocytes. Slc26a2 expression was manipulated acutely by delivery of Slc26a2 or shSlc26a2 with lentiviral vectors. We demonstrate that slc26a2 is essential for chondrocyte proliferation and differentiation and for proteoglycan synthesis. Slc26a2 also regulates the terminal stage of chondrocyte cell size expansion. These findings reveal multiple roles for Slc26a2 in chondrocyte biology and emphasize the importance of Slc26a2-mediated protein sulfation in cell signaling, which may account for the complex phenotype of DTD.

Mammalian skeletal development is a tightly regulated process, central to which are the chondrocytes that form all bone types (1, 2). Chondrocytes are derived from mesenchymal progenitor cells. Bone formation is initiated when activation of cartilage-specific genes causes mesenchymal cell condensation and differentiation into chondrocytes (3). These chondrocytes form a cartilaginous template using abundant extracellular matrix (ECM)[3] comprised of proteoglycans. The ECM surrounds mature chondrocytes and mediates cell-cell contacts (3, 4).

Long bone elongation requires chondrocyte proliferation, differentiation, and secretion of ECM to form the growth plate cartilage (3). The growth plate is divided into three distinct zones: the resting, proliferating, and mineralization zones (5). In the resting zone, the chondrocytes, which are non-polarized and arranged irregularly, serve as a committed stem cell pole. These relatively immature cells differentiate into rapidly dividing and proliferating chondrocytes in the proliferating zone. In the hypertrophic zone, chondrocyte proliferation ceases, and matrix ossification/mineralization starts.

Bone growth and homeostasis are highly regulated by multiple factors, the most prominent of which are members of the TGF-β and insulin-like growth factor 1 (IGF-1) families (6). IGF-1 has an essential role in longitudinal bone growth because *Igf1* gene deletion causes dwarfism in mice (7), and aberrant IGF-1 signaling leads to extremely short stature in humans (8) due to impaired chondrocyte hypertrophy. Recent studies have reported that chondrocyte hypertrophy occurs in three phases. IGF-1 regulates the third phase to promote longitudinal bone growth (9). The mechanism by which chondrocytes become hypertrophic without adding cell mass must involve osmolyte transport. However, the details of this process are poorly understood, including the electrolyte transporters mediating chondrocyte hypertrophy and the role of IGF-1.

Slc26a2 is a transporter with essential role in bone formation, which may also participate in chondrocyte volume expansion. We have shown recently that Slc26a2 functions as a $SO_4^{2-}/Cl^-/OH^-$ exchanger that is exquisitely regulated by extracellular Cl^- (10). Mutations in Slc26a2 cause diastrophic dysplasia

* This work was supported, in whole or in part, by National Institutes of Health Intramural Grant ZIA DE000735. This work was also supported by National Research Foundation Grants NRF-2008-359-C00029 and NRF-2009-0071060] and MSIP Grant 2013R1A2A1A01011908 funded by the Korean government.

[1] To whom correspondence may be addressed: E-mail: parkjh@sookmyung.ac.kr.
[2] To whom correspondence may be addressed: E-mail: shmuel.muallem@nih.gov.

[3] The abbreviations used are: ECM, extracellular matrix; IGF, insulin-like growth factor; DTD, diastrophic dysplasia; qPCR, quantitative PCR; MAC, mouse articular chondrocyte; Col-II, type II collagen; E11.5, embryonic day 11.5; pHi_i, intracellular pH; P0, passage 0.

(DTD), a disorder of cartilage and bone development characterized by growth retardation, skeletal dysplasia, and joint contracture (11, 12). The skeletal phenotype is typified by reduction of cartilage, irregular chondrocyte size, delayed secondary ossification center formation, and osteoporosis of the long bones. Moreover, reduced chondrocyte proliferation and lack of terminal differentiation likely contribute to reduced bone growth in DTD (11, 13, 14). Thus, the growth plate height and the number of cartilage-forming chondrocytes are greatly reduced in the Slc26a2 mutant mouse (15). These findings suggest that, in addition to its known role in cartilage protein sulfation, Slc26a2 has multiple roles in chondrocyte biology.

In this work, we set out to determine the role of Slc26a2 in chondrocyte function using two distinct cartilage model systems. The first is a mouse embryonic limb bud mesenchymal cell system. Upon stimulation with serum, mesenchymal cells undergo condensation, followed by proliferation and differentiation to chondrocytes, and, finally, maturation to hypertrophic chondrocytes after several days in culture. The second system is a murine articular chondrocyte system. Chondrocytes are isolated from the femoral head, femoral condyle, and tibial plateau of 5-day-old pups and differentiated into hypertrophic chondrocytes by serial passages. We also determined the role of Slc26a2 in IGF-1-dependent chondrocyte maturation and proteoglycan synthesis. We found that Slc26a2 expression is highly enriched in the long bone proliferating zone. Knockdown and overexpression of Slc26a2 revealed an essential role of Slc26a2 in chondrocyte differentiation and maturation. Moreover, Slc26a2 function is required for proteoglycan synthesis, cartilage formation, and sulfation. IGF-1 acutely stimulates Slc26a2 activity through activation of the PI3K pathway to stimulate ECM formation and chondrocyte size expansion. These findings demonstrate, for the first time, the multiple roles of Slc26a2 in chondrocyte function and bone formation.

MATERIALS AND METHODS

Mice—Mice were purchased from Charles River Laboratories Japan. All mouse experiments were performed according to the guidelines of the Animal Care and Use Committee of Sookmyung Women's University.

Plasmids, Reagents, and Solutions—The murine slc26a2 (IMAGE ID 4014785) was from Source BioScience and was cloned into the pcDNA3.1(+) vector using the HindIII and XhoI sites. Anti-Slc26a2 polyclonal antibodies were generated by Cosmogenetech. Rabbit Slc26a2 polyclonal antibodies were generated against keyhole limpet hemocyanin (KLH)-conjugated synthetic Slc26a2 peptide (KELNEHFKDKLKA). Anti-β-actin antibodies were from Sigma-Aldrich. IGF-1 was from Sigma-Aldrich, and LY-294002, LY-303511, and PI828 were from R&D Systems. 2′7′-bis-(2-carboxyethyl)-5-(and-6)-carboxyfluorescein and F-125 were purchased from Molecular Probes. siRNA directed against the PI3K p85β subunit was purchased from Santa Cruz Biotechnology. DMEM and Hanks' buffered salt solution were from Invitrogen. For measurement of pH_i, the standard bath solution contained 140 mM NaCl, 5 mM KCl, 1 mM $MgCl_2$, 1 mM $CaCl_2$, 10 mM HEPES, and 10 mM glucose (pH 7.4 with NaOH). The Cl^--free solution contained 140 mM sodium gluconate, 5 mM potassium gluconate, 10 mM HEPES, 1 mM calcium gluconate, 1 mM magnesium gluconate, and 10 mM glucose (pH 7.4). Where indicated, the Cl^--free solution also included 5 mM Na_2SO_4.

RT-PCR, shRNA, siRNA, and qPCR—Total RNA was extracted using TRIzol reagent (Invitrogen) according to the instructions of the manufacturer. For RT-PCR, 1 μg of total RNA was reverse-transcribed into single-strand cDNA using the anchored oligo(dT) primer and M-MLV reverse transcriptase (Invitrogen). Primers for RT-PCR were as follows: Slc26a2, 5′-TCC ATC ATT ACT TTG CAG ATG G-3 (forward) and 5′-CCT GAG AAT GAC ACC CCA GT-3′ (reverse); 152-bp Col-II, 5′-CAC ACT GGT AAG TGG GGC AAG A-3′ (forward) and 5′-GGA TTG TGT TGT TTC AGG GTT CG-3′ (reverse); 173-bp MMP13, 5′-TGA TGG ACC TTC TGG TCT TCT GG-3′ (forward) and 5′-CAT CCA CAT GGT TGG GAA GTT CT-3′ (reverse); 473-bp GAPDH, 5′-TCA CTG CCA CCC AGA AGA C-3′ (forward) and 5′-TGT AGG CCA TGA GGT CCA C-3′ (reverse); and 450-bp GAPDH was used as a control. siRNA directed against the PI3K p85β subunit was purchased from Santa Cruz Biotechnology.

shRNAs were obtained from Open Biosystems. The knockdown efficiency of the Slc26a2 shRNA was determined by RT-PCR, and the most efficient corresponded to hairpin sequence shRNA-Slc26a2_#1 (5′-CCG GGC TCT TTA TTC TAT TCC CTT CTC GAG AAG GGA ATA GAA TAA AGG AGC TTT TG-3′) and shRNA-Slc26a2_#2 (5′-CCG GCC TCT CTA CTA CAT AAA CAA ACT CGA GTT TGT TTA TGT AGT AGA GAG GTT TTG-3′). Scrambled shRNA was obtained from Addgene (5′ CCT AAG GTT AAG TCG CCC TCG CTC TAG CGA GGG CGA CTT AAC CTT AGG-3′). shRNA-Slc26a2 and scrambled shRNA were transfected into murine articular chondrocytes (MAC) using FuGENE 6 as described in the protocol of the manufacturer. Confirmation of shRNA knockdown by RT-PCR and immunoblotting was carried out in murine articular chondrocytes. For qPCR, 1 μg of total RNA was reverse-transcribed using the same conditions as above. 1/10 dilutions were used in triplicate with 0.2 μM primer and 5 μl of LightCycler 480 SYBR Green I Master in a 10-μl reaction, and qPCR was executed in a 384-well block on a Light Cycler 480 system (Roche). Expression levels were normalized to endogenous expression of GAPDH. Fold changes were calculated using the $\Delta\Delta C_t$ method according to the instructions of the manufacturer.

Lentiviral Infection—Lentiviruses were produced from Macrogen. The titer was $\sim 10^7 \sim 10^8$ transduction units/ml and was used without further concentration. One day after plating, cells at 3×10^5/spot and with monolayers at 4×10^5 cells/dish were infected with a multiplicity of infection of 50 of lenti-Slc26a2 or lenti-shRNA-Slc26a2 with 5 μg/ml of Polybrene. After 2 days, the medium was changed, and the cells were treated with the indicated experimental protocols.

BrdU Incorporation Assay—The cells were incubated in culture medium containing 10 μM BrdU (Sigma) for 4 h, washed with PBS, and fixed with 4% paraformaldehyde. DNA was denatured by incubation with 1.5 M HCl for 20 min and subsequent neutralization with 0.5 M sodium borate. The cells were blocked and permeabilized by incubation with 5% serum containing 0.2% Triton X-100 prior to addition of primary antibody. BrdU

labeling was detected using an anti-BrdU antibody (Sigma) and Alexa Fluor 594 goat anti-mouse IgG antibody (Invitrogen) and counterstained with DAPI (Sigma).

Micromass Culture of Embryonic Limb Mesenchymal Cells—Culture- and time-dependent differentiation of mesenchymal cells in culture were prepared as described in Ref. 16, with small modifications as follows. Embryonic limb mesenchymal cells were isolated from the limb buds of E11.5 embryos and allowed to undergo condensation, giving rise to the formation of cartilaginous nodules that consisted of sulfated proteoglycans. One-third of the limb buds of E11.5 embryos were microdissected and washed with Hanks' buffered salt solution and digested with collagen D for 10 min at 37 °C. Digestion was terminated by the addition of the same volume of DMEM supplemented with 10% FBS, 50 μg/ml streptomycin, and 50 units/ml penicillin. The digest was filtered through a sterile 20-μm cell strainer to isolate the mesenchymal cells. Mesenchymal cells were spotted on a culture dish at a density of 3×10^5/spot. Four hours after spotting, medium was added to cover the spots. One day after spotting the cells, the culture medium was changed, and the cells were infected with lenti-shRNA-Slc26a2 or lentiviral Slc26a2 in the presence or absence of 100 ng/ml IGF-1. After 5 days in culture in the presence of 10% serum, maximal differentiation of chondrocytes and matrix formation was achieved. At this stage, cartilaginous nodule formation was analyzed by Alcian blue staining, which stains the highly sulfated proteoglycans and reveals their synthesis. For cartilage organ culture, cartilage was isolated from the femoral heads and tibias of 5-day-old mice and grown in DMEM with 10% FBS, 50 μg/ml streptomycin, and 50 units/ml penicillin for 4 days.

Monolayer Culture and Three-dimensional Pellet Culture of MACs—MACs in primary culture were prepared from the cartilage of the femoral heads and tibias of 5-day-old mice. The cartilage was incubated with 1% collagenase D for 4 h. Collagenase digestion was terminated by addition of the same volume of medium containing 10% serum (DMEM, 10% FBS, 50 μg/ml streptomycin, and 50 units/ml penicillin). Cells were collected by centrifugation and washed twice with Hanks' buffered salt solution. The pellet was resuspended, and cells were seeded as a monolayer on a culture dish. The medium was changed every 2 days. Starting on the first day, cells were subjected to serial passage from passage 0 to passage 2 every 5 days.

For generating three-dimensional pellet cultures, 24 h after seeding mouse articular chondrocytes, the cells were trypsinized, counted, and then 4×10^5 cells were pipetted into 15-ml tubes. Cells were centrifuged at $460 \times g$ for 10 min and the supernatant was decanted. The pellets were carefully layered with 1 ml of culture medium, and the tubes were incubate in a CO_2 incubator. The next day, the cells were infected with lenti-Slc26a2 or lenti-shRNA-Slc26a2 and treated with vehicle or 100 ng/ml IGF-1 as specified. The medium was changed every 2 days for 7 days. The pellets were then washed with PBS twice, and the cells were fixed by the addition of 1 ml 4% paraformaldehyde and rocking for 2 h. The pellets were air-dried, detached from the 15-ml tube, and then the pellet was embedded in OCT (optimum cutting temperature) compound. Cryostat sections were stained with Alcian blue and imaged.

Alcian Blue Staining—For evaluation of sulfated proteoglycan synthesis, cells were fixed with solution containing 30% EtOH, 0.4% paraformaldehyde, and 4% acetic acid for 15 min at room temperature and stained with 1% Alcian blue 8GS (Sigma) at pH 1.0 overnight to specifically stain the sulfated proteoglycans. For quantification of sulfated proteoglycan synthesis, Alcian blue-stained cells were washed three times with double-distilled water, and the cells were extracted with 6 M guanidine hydrochloride by overnight incubation with gentle shaking. The absorbance of the released dye was measured at 656 nm.

Analysis of Mouse Articular Chondrocyte Cell Size—Cultures of mouse articular chondrocytes treated as indicated were photographed using an Olympus DP73 camera. The images were imported into ImageJ 1.45s (NIH Image Core Development), and the cell size was analyzed. The entire images were selected, and a threshold was applied to highlight the cell edges. The average cell sizes were then determined by the software for each image. Multiple images from each culture were captured randomly and averaged to obtain the mean ± S.E.

Measurement of Slc26a2 Activity—HeLa cells grown on coverslips that formed the bottom of a perfusion chamber were cotransfected with Slc26a2 and/or siPI3K and GFP. Two days after transfection, the cells were loaded with the pH-sensitive dye 2′7′-bis-(2-carboxyethyl)-5-(and-6)-carboxyfluorescein (2.5 μM) and F-125 for 10 min and washed by perfusion with standard bath solution to remove external dyes and allow recovery of the resting pH. Cells were then treated with vehicle or 100 ng/ml IGF-1 for 10 min in the absence or presence of PI828 or Ly294002. The fluorescence ratio of 490/440 nm was monitored by a PTI system, and the ratio was used to determine changes in pH_i as described before (17).

Measurement of $^{35}SO_4^{2-}$ Uptake—MACs and HeLa cells were washed with PBS and then incubated in low ionic buffer (1 mM $MgCl_2$, 300 mM sucrose, and 10 mM Tris-HEPES (pH 7.4)) and 0.5 mM SO_4^{2-} supplemented with 5 μCi/ml $^{35}SO_4^{2-}$ at 37 °C. After 10 min of incubation, the uptake reaction was terminated by washing the cells three times with ice-cold washing buffer (containing 100 mM sucrose, 100 mM NaN3, 1 mM $MgCl_2$, and 10 mM Tris-HEPES), denatured with 10% trichloroacetic acid, and solubilized with a solution containing 1N NaOH and 2% SDS. Uptake was calculated as pmol/10^5 cells/min.

Statistics—All experiments were repeated at least three times, and the results are given as mean ± S.E. Statistical analysis was performed using Prism software. Differences between the groups were analyzed for statistical significance by Student's *t* test. $p < 0.05$ was considered statistically significant.

RESULTS

Slc26a2 Expression Level Correlates with Mesenchymal Cell Differentiation to Chondrocytes—Bone formation starts with the laying down of cartilage by chondrocytes, which is comprised primarily of sulfated proteoglycans (4). Proteoglycan sulfation depends on SO_4^{2-} uptake by chondrocytes. The SO_4^{2-} transporter Slc26a2 mediates most SO_4^{2-} uptake by chondrocytes, as evident from the reduced sulfation of cartilage of patients with DTD (18) and of the DTD mouse (11). We have shown recently that Slc26a2 functions as a $SO_4^{2-}/Cl^-/OH^-$

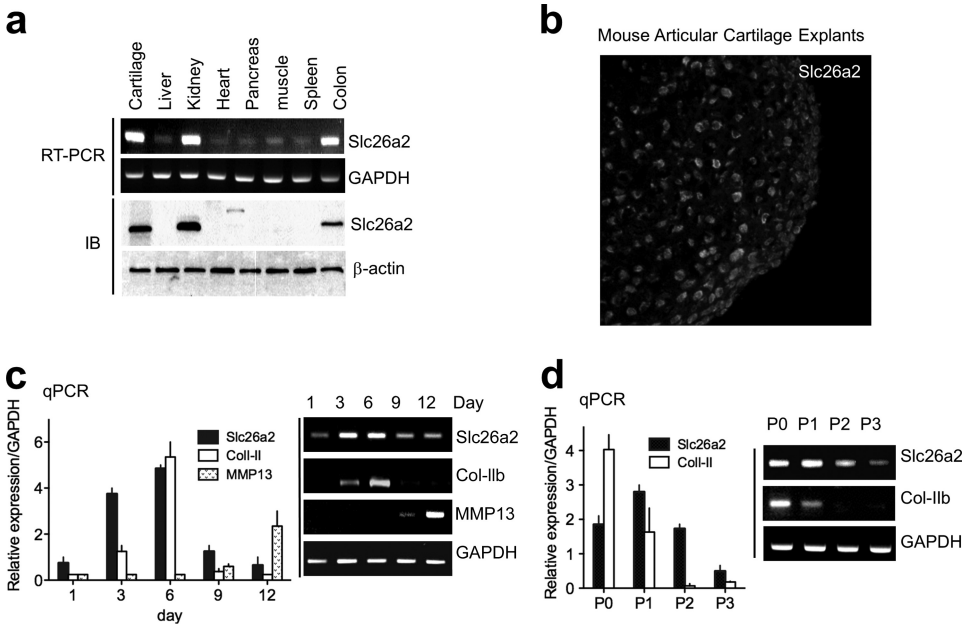

FIGURE 1. **Expression pattern of the $SO_4^{2-}/Cl^-/OH^-$ exchanger Slc26a2.** *a*, the indicated mouse tissues were used to analyze Slc26a2 mRNA by RT-PCR and protein by Western blot analysis. *IB*, immunoblot. *b*, immunolocalization of Slc26a2 in chondrocytes from mouse articular cartilage explants. *c* and *d*, changes in Slc26a2 mRNA during chondrocyte differentiation and maturation that were measured as a function of time in culture (*c*) and during cell passages (*d*). Col-II was used as the marker for proliferating chondrocytes and MMP13 as the marker for terminal chondrogenesis of hypertrophic chondrocytes in micromass culture of embryonic limb mesenchymal cells. Expression was analyzed by qPCR (*columns*) and RT-PCR (*blots*). The results are given as mean ± S.E. of three independent experiments.

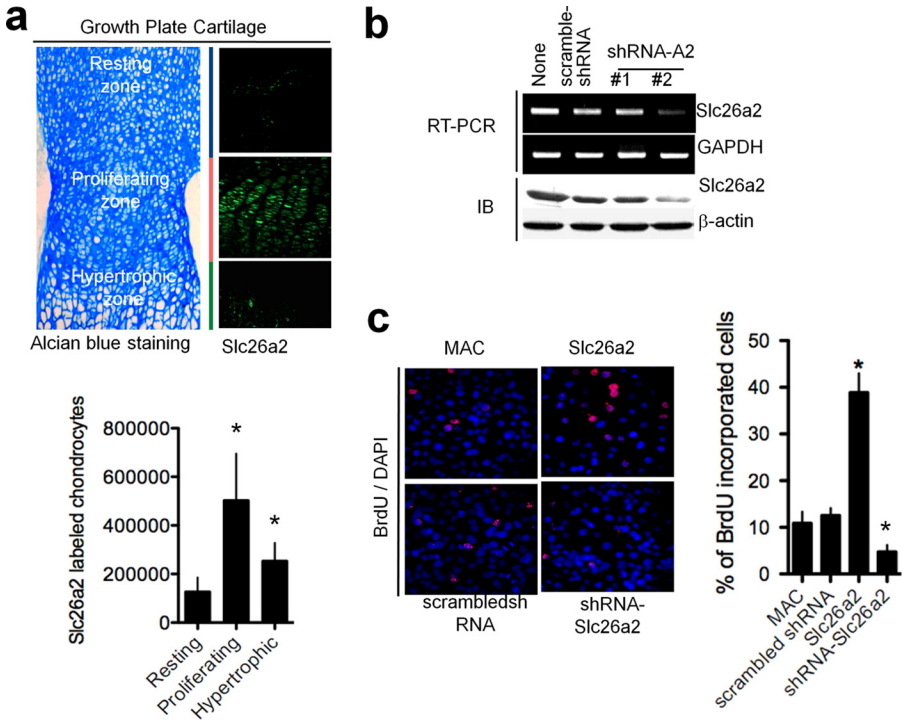

FIGURE 2. **Slc26a2 stimulates chondrocyte proliferation.** *a*, localization of Slc26a2 in a 5-day-old mouse epiphyseal growth plate. Growth plate zones were identified by Alcian blue staining, and the number of chondrocytes expressing Slc26a2 in each zone was determined using ImageJ software (*columns*). The averages are the mean ± S.E. of four experiments. *b*, shRNA #2 reduced the expression of Slc26a2 mRNA and protein in MACs by about 70% after 72 h of treatment. *IB*, immunoblot. *c*, expression of Slc26a2 increased, whereas knockdown of Slc26a2 decreased, proliferation of MACs. Cells were treated with Slc26a2 and shSlc26a2 for 2 days before an assay of cell proliferation by BrdU staining ($n = 3$). *, $p < 0.05$.

exchanger that is regulated by external Cl^- (10). However, the multiple skeletal abnormalities in DTD, including reduced cartilage volume, irregular chondrocyte size, reduced chondrocyte proliferation, and lack of terminal chondrocyte differentiation (11, 13, 14), suggest that Slc26a2 may have additional roles in chondrocyte biology.

To further understand the role of Slc26a2 in chondrocyte function, we first followed Slc26a2 expression during chondro-

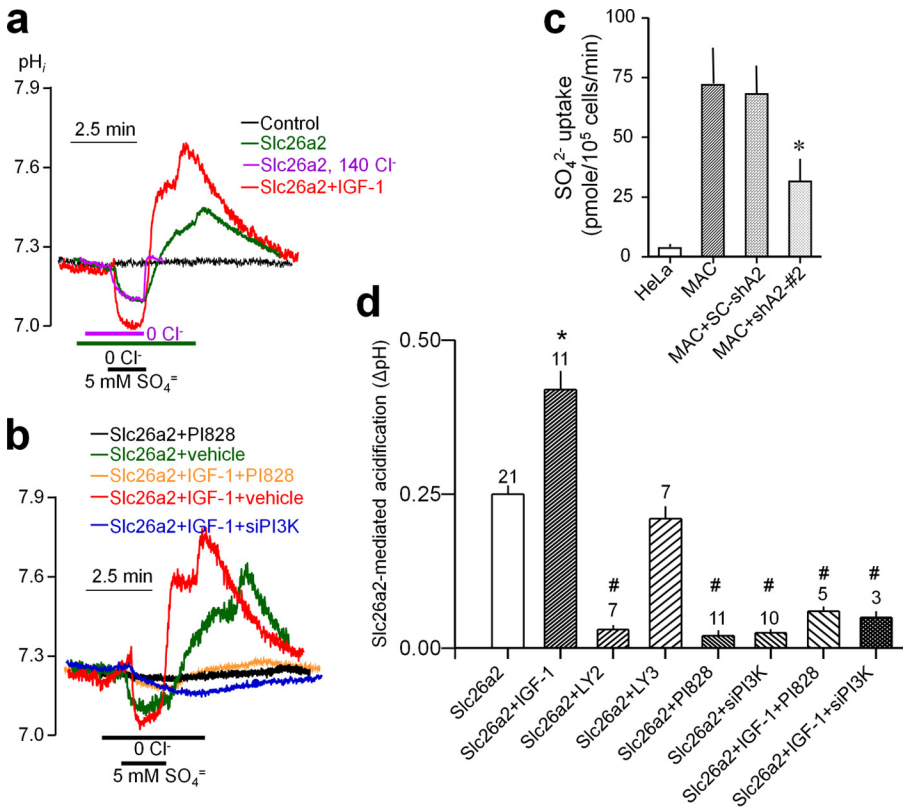

FIGURE 3. **IGF-1 activates Slc26a2 through the PI3K pathway.** *a* and *b*, example traces. *d*, summary of the number of experiments indicated on top of the *columns*. Slc26a2 activity was measured in transfected HeLa cells as the reduction of pH_{in} changes in response to exposing the cells to 5 mM SO_4^{2-} in a Cl^--free solution. HeLa cells expressing Slc26a2 were treated with vehicle of 100 ng/ml IGF-1 for 10 min before measurement of pH_{in}. Treatment with the PI3K inhibitors was for 10 min prior to measurement of pH_i. The concentrations used were 10 μM Ly294002, 20 μM LY303511, and 2.5 μM PI828. Cells were also treated with PI3K siRNA or scrambled (SC) siRNA for 48 h prior to transfection of Slc26a2 and measurement of pH_{in} 24 h later. *c*, measurement of $^{35}SO_4^{2-}$ uptake into MACs, MACs treated with shSlc26a2, and untransfected HeLa cells as controls. *, $p < 0.05$; #, $p < 0.01$ relative to the respective controls. In *c*, the control is SO_4^{2-} uptake by MACs. In *d*, the control is the acidification measured in unstimulated cells expressing Slc26a2.

cyte differentiation using two model systems. The RT-PCR analysis and Western blotting in Fig. 1*a* show the ubiquitous expression of Slc26a2, with a high expression of Slc26a2 in the cartilage, kidney, and colon. Fig. 1*b* shows expression of Slc26a2 in chondrocytes of freshly isolated mouse articular cartilage explants. In Fig. 1*c*, we used micromass culture of embryonic limb mesenchymal cells that were allowed to differentiate over 12 days in culture. Expression of Col-II was used as a marker for proliferating chondrocytes, (19), and expression of MMP13 was used as a marker for terminally differentiated hypertrophic chondrocytes (20). qPCR (*columns*) and RT-PCR (*blots*) showed that the expression levels of Slc26a2 followed that of Col-II (Fig. 1*c*). This was confirmed by determining the expression patterns of Col-II and Slc26a2 in cultured MACs that had been differentiated by serial passages (Fig. 1*d*).

High Slc26a2 Expression in Proliferating Chondrocytes Is Required for MAC Proliferation—The findings in Fig. 1, *c* and *d*, suggest a high expression of Slc26a2 in proliferating chondrocytes. To further probe the role of Slc26a2 in chondrocyte proliferation, we determined Slc26a2 expression in mouse epiphyseal growth plates (Fig. 2*a*). The growth plate cartilage was stained with Alcian blue to demarcate morphological differences among zonal chondrocytes. Fig. 2*a* shows high Slc26a2 expression in the proliferating zone, modest expression in the hypertrophic zone, and minimal expression in the resting zone. Evidence for a possible role of Slc26a2 in chondrocyte proliferation is shown in Fig. 2, *b* and *c*. Fig. 2*b* shows that 72 h of treatment with Slc26a2 shRNA #2 decreased mRNA and protein expression of Slc26a2 in cultured MACs by about 70%. In Fig. 2*c*, MAC proliferation was analyzed by BrdU assay. MACs in culture were transfected either with empty vector, scrambled shRNA, shSlc26a2, or Slc26a2, and proliferation was evaluated by staining the cells for BrdU. Counting the BrdU-positive cells in multiple, randomly selected fields in four different experiments showed that expression of Slc26a2 increased MAC proliferation, whereas knockdown of Slc26a2 significantly decreased MAC proliferation (Fig. 2*c*). This is further supported by the finding that, in the DTD knock-in mouse, there is a reduction in both chondrocytes and BrdU-positive cells in the proliferating zone of the long bone growth plate (13).

Activation of Slc26a2 by IGF-1—The IGF-1 pathway potently regulates chondrocyte function by regulating sulfated proteoglycan synthesis (21, 22) and the critical step of chondrocyte size expansion (9). To study the role of Slc26a2 in IGF-1-mediated chondrocyte regulation, we first determined the effect of IGF-1 stimulation on Slc26a2 activity in HeLa cells, which express native IGF-1 receptors (23) and have minimal Slc26a2 activity. Slc26a2 activity was measured by following intracellular pH (pH_i) to record the SO_4^{2-}/OH^- exchange activity. The experimental protocol and basal activity of HeLa cells transfected with empty vector (*black trace*) and Slc26a2 (*green trace*) are shown in Fig. 3*a*. Cells bathed in HEPES-buffered

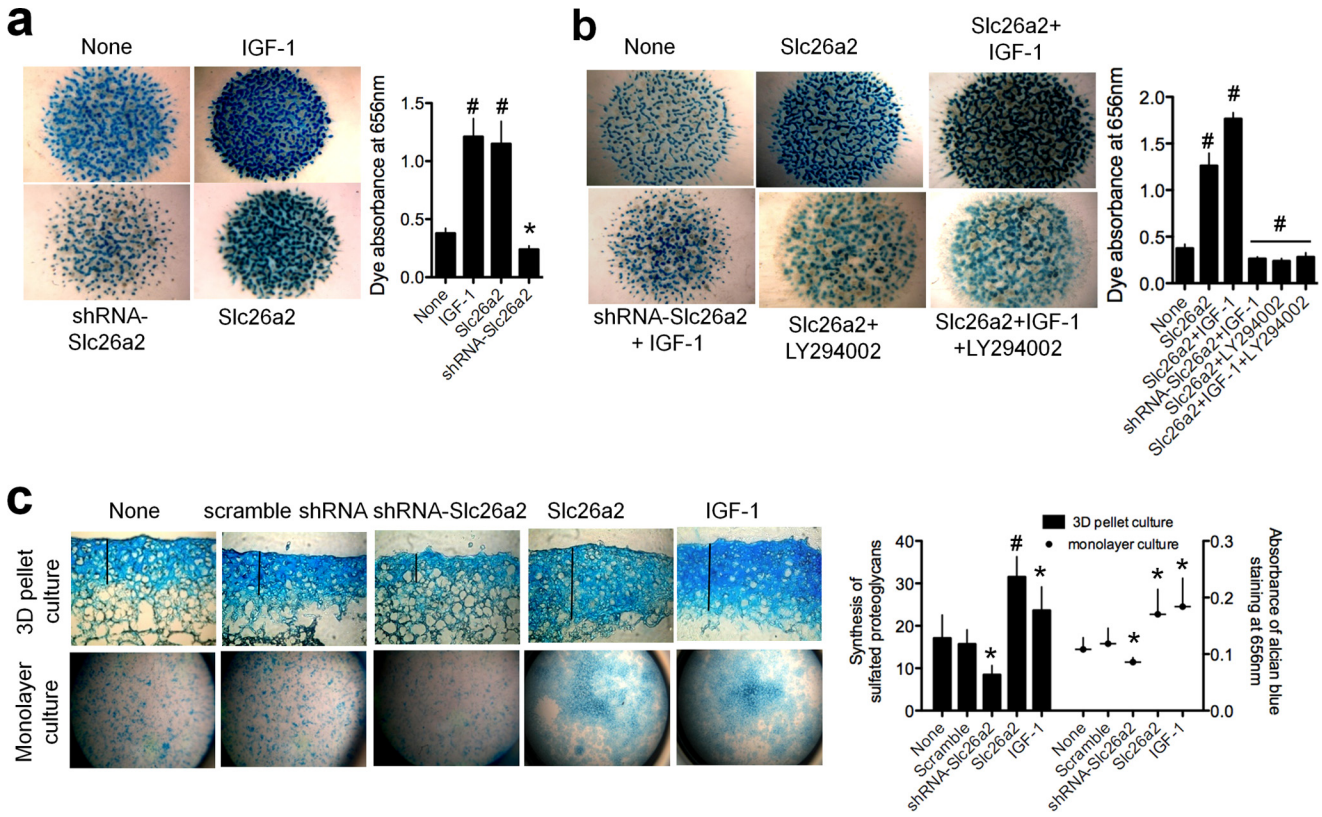

FIGURE 4. **Slc26a2 is essential for proteoglycan synthesis by chondrocytes.** *a* and *b*, micromass cultures of embryonic limb mesenchymal cells were prepared from limb buds of E11.5 embryos and allowed to undergo condensation to form cartilaginous nodules consisting of sulfated proteoglycans. Infection with lentiviruses carrying Slc26a2 and shSlc26a2 were as described under "Materials and Methods." The cultures were treated with vehicle (dimethyl sulfoxide), 10 μM of the PI3K inhibitor LY29002, or 100 ng/ml IGF-1. At the end of the incubation, the micromasses were stained with Alcian blue to visualize the sulfated proteoglycans. In *a*, the controls are micromasses without any treatment. In *b*, the controls are micromasses treated with dimethyl sulfoxide. The results are representative of three to four experiments, and the columns show the mean ± S.E. *c*, three-dimensional (*3D*) cultures ($n = 4–5$) and a monolayer culture ($n = 3$) of mouse articular chondrocytes were prepared as detailed under "Materials and Methods," infected with Slc26a2 or shSlc26a2, and treated with 100 ng/ml IGF-1. The controls were cultures without any treatment. After 5 days in culture, sulfated proteoglycans were analyzed by staining with Alcian blue and measurements of the Alcian blue absorbance. Shown are representative images, and the columns are mean ± S.E. *, $p < 0.05$; #, $p < 0.01$ relative to the respective untreated controls (*None*).

medium were perfused with Cl^--free solution and then exposed to a Cl^--free solution containing 5 mM SO_4^{2-}. This resulted in acidification because of SO_4^{2-} influx and OH^- efflux. Removal of external SO_4^{2-} slowly reversed the change in pH_i and resulted in an overshoot of pH_i. Restoring bath Cl^- resulted in recovery of pH_i because of Cl^-/OH^- exchange. The overshot is likely due to hidden $Cl^-{}_{in}/SO_4^{2-}{}_{out}$ exchange during $SO_4{}^{2-}$ uptake and $SO_4^{2-}{}_{in}/OH^-{}_{out}$ exchange during the incubation in Cl^--free solution. Accordingly, Fig. 3*a* (*magenta trace*) shows that, in the presence of external Cl^-, the overshoot is nearly eliminated.

Attempts to demonstrate Slc26a2 activity in MACs using the pH_i assay resulted in a small signal. Alternatively, we measured $^{35}SO_4^{2-}$ uptake in MACs and used untransfected HeLa cells as a control. Fig. 3*c* shows that $^{35}SO_4^{2-}$ uptake by MACs is much higher than that in HeLa cells and is reduced by about 65% when MACs are treated with shSlc26a2.

The effect of IGF-1 on Slc26a2 function was then studied in HeLa cells expressing Slc26a2. Notably, IGF-1 activated Slc26a2 (Fig. 3, *a* and *d*). This is evident from the faster rate and larger extent of reduction in pH_i on exposure to SO_4^{2-} and increase in pH_i on removal of SO_4^{2-}. The function of IGF-1 in chondrocytes is mediated by the PI3K pathway (24), although the targets of IGF-1 and PI3K are not well defined. Therefore, we used several probes to test the role of the PI3K pathway in IGF-1-mediated activation of Slc26a2. Unexpectedly, as seen in Fig. 3, *b* and *d*, the PI3K inhibitors Ly294002 and PI828 and siRNA knockdown of PI3K all markedly reduced the activity of Slc26a2 in unstimulated cells, as well as in cells stimulated with IGF-1. This indicates that the PI3K is obligatory for the function of Slc26a2.

Slc26a2 Regulates Sulfated Proteoglycan Synthesis—The essential role of IGF-1 in proteoglycan synthesis (6) and the regulation of Slc26a2 by IGF-1 (Fig. 3) raised the question of whether Slc26a2 function is required for proteoglycan synthesis. This was tested using micromass culture of embryonic limb mesenchymal cells isolated from limb buds of E11.5 embryos. These cells undergo condensation and differentiation giving rise to formation of cartilaginous nodules consisting of sulfated proteoglycans that can be analyzed by staining with Alcian blue. Fig. 4*a* shows that treating the chondrocytes with 100 ng/ml IGF-1 markedly increased proteoglycan synthesis. Surprisingly, overexpression of Slc26a2 was almost as effective as IGF-1 in increasing proteoglycan synthesis and knockdown of Slc26a2 prominently reduced basal proteoglycan synthesis. Moreover, Fig. 4*b* shows that knockdown of Slc26a2 strongly inhibited the

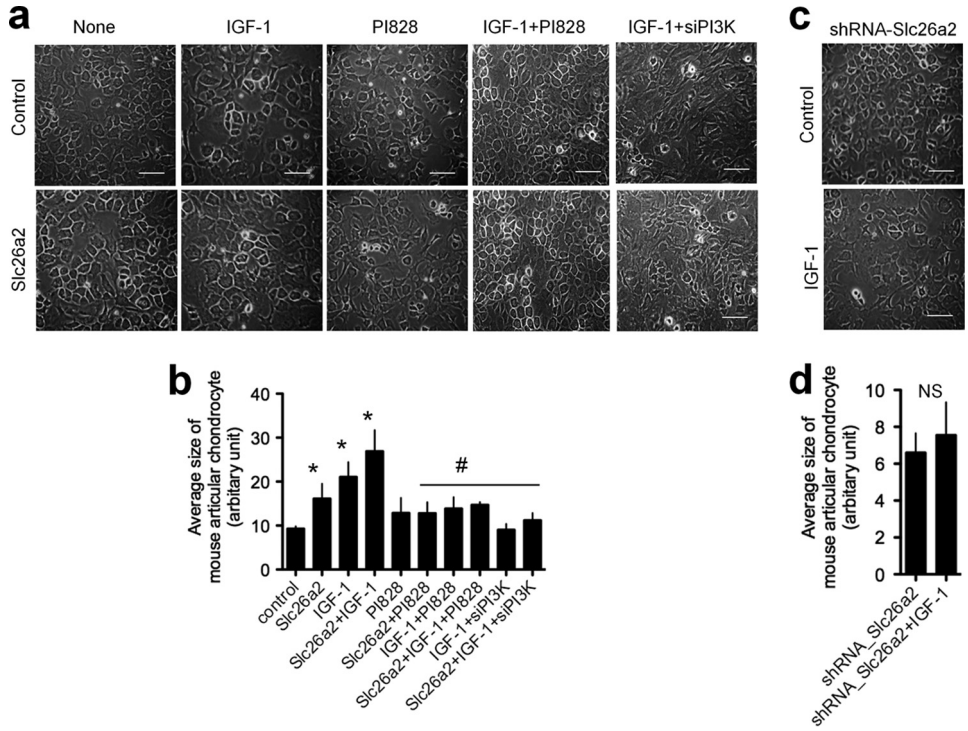

FIGURE 5. **Slc26a2 is essential for chondrocytes size increase.** Mouse articular chondrocytes in culture were passed until passage P2 and then transfected with an empty vector (*Control*), Slc26a2 (*a* and *b*), or shSlc26a2 (*c* and *d*). Two days after transfection, the cells were treated with 100 ng/ml IGF-1 (*a–d*) in the presence of absence of the PI3K inhibitor PI828 (*a* and *b*) and incubated for an additional 3 days. At the time of transfection with Slc26a2, cells were also treated with siPI3K (*a* and *b*). After a total of 5 days, cell sizes were analyzed by ImageJ as described under "Materials and Methods." *Scale bars*, 30 μm. The columns show the averages of three to five experiments. *, $p < 0.05$; #, $p < 0.01$ relative to the respective controls; *NS*, not significant. For *b* and *d*, the control was untreated cells, marked as *control* in *b*.

effect of IGF-1 on proteoglycan synthesis, and IGF-1 had a very modest effect on proteoglycan synthesis in cells overexpressing Slc26a2. As expected, inhibition of PI3K by Ly294002 inhibited the effects of both Slc26a2 and IGF-1.

To provide further support for these findings, we measured proteoglycan synthesis by mouse articular chondrocytes that were maintained either in three-dimensional culture (Fig. 4*c*, *top row* and *columns*) or in monolayer culture (*bottom row* and *symbols*). Again, treatment with IGF-1 and overexpression of Slc26a2 increased proteoglycan synthesis, whereas knockdown of Slc26a2 inhibited synthesis. The findings in Fig. 4 indicate that IGF-1 and Slc26a2 function in the same metabolic pathway; that the activity of Slc26a2 is essential for proteoglycan synthesis, not only sulfation; and that Slc26a2 is essential for IGF-1-mediated stimulation of proteoglycan synthesis.

Slc26a2 Regulates Chondrocytes Cell Size—Another well defined function of IGF-1 is the stimulation of chondrocyte volume expansion (9) by an unknown mechanism. Therefore, we determined whether Slc26a2 affects chondrocyte cell size and whether it is required for an IGF-1-mediated increase in chondrocytes size. In Fig. 5, MACs at serial passage 2 were transfected with empty vector or with Slc26a2. Two days after transfection, the cells were treated with IGF-1 in the presence or absence of the PI3K inhibitor PI828 or treated with siPI3K and incubated for an additional 3 days. IGF-1 and Slc26a2 increased chondrocyte size with a combined effect smaller than the additive effect. PI3K activity was necessary for both IGF-1-mediated and Slc26a2-mediated chondrocyte volume expansion.

DISCUSSION

This study aimed to explore the role of the $SO_4^{2-}/Cl^-/OH^-$ exchanger Slc26a2 in key chondrocyte functions essential for bone metabolism. Mutations in Slc26a2 are associated with DTD (25), and features of the disease are generally attributed to lack of SO_4^{2-} transport needed for sulfation of ECM proteins. However, DTD is characterized by other aberrant functions of chondrocytes, including reduction in cartilage, irregular chondrocyte size, reduced chondrocyte proliferation, and lack of terminal chondrocyte differentiation. These are unlikely to result solely from defective proteoglycan sulfation (11, 13, 14).

To further study the role of Slc26a2 in chondrocyte function, we changed Slc26a2 expression acutely to minimize the compensation and adaptation that may occur in murine models of DTD and to examine the role of Slc26a2 overexpression. In addition, acute manipulation in culture allowed us to follow the dynamic regulation of chondrocyte function. Of note, the reduced Slc26a2 activity in the mouse model of DTD (13) and knockdown of Slc26a2 in chondrocytes (Fig. 2) showed a similar impairment in chondrocyte proliferation. This suggests that the function of Slc26a2 in chondrocytes cannot be compensated for by any of the other SLC26 SO_4^{2-} transporters, such as the ubiquitous Slc26a1 and slc26a6 or Slc26a3 (27, 28).

Chondrocytes are regulated by multiple growth factors, principally members of the TGFβ and FGF superfamilies, which

affect chondrocyte proliferation, differentiation, and ECM synthesis (6, 29). However, IGF-1 is a key growth factor in skeletal development that also influences the effect of TGF-β receptors (6, 30). Therefore, we focused on the role of Slc26a2 in regulation of chondrocytes by IGF-1. Interestingly, knockdown of Slc26a2 inhibited the effects of IGF-1, and overexpression of Slc26a2 recapitulated the effects of stimulation with IGF-1. Importantly, IGF-1 minimally increased proteoglycan synthesis and chondrocyte size in cells overexpressing Slc26a2, suggesting that many effects of IGF-1 are mediated by increased Slc26a2 activity and, perhaps, expression (31).

Our findings suggest that the PI3K pathway is essential for basal Slc26a2 activity and for stimulation of Slc26a2 by IGF-1 (Fig. 3). The requirement of PI3K activity for the basal activity of Slc26a2 was unexpected and was observed with two independent PI3K inhibitors and by knockdown of PI3K. This suggests that Slc26a2 is constitutively phosphorylated by PI3K. Considering the central role of Slc26a2 in chondrocyte biology, our findings indicate a major role for PI3K in regulation of chondrocytes (29). Interestingly, inhibition of basal PI3K activity inhibits basal growth and the effects of parathyroid hormone, C-type natriuretic peptide, and IGF-1 in explant cultures (32–34). In addition, expression of active Akt in murine cartilage promotes chondrocyte differentiation, whereas dominant-negative Akt delays chondrocyte differentiation (35). Our findings of regulation of both basal and stimulated Slc26a2 activity by PI3K is consistent with and can explain these findings. Furthermore, it is likely that Slc26a2 mediates the function of other agonists acting on chondrocytes through the PI3K pathway.

Our findings support a more general role of Slc26a2 in chondrocyte development and function than has been appreciated previously. Slc26a2 influences chondrocyte proliferation (Fig. 2), differentiation (Fig. 4), and growth (Fig. 5). How can Slc26a2 mediate such a variety of chondrocyte functions? This may be related to the multiple roles of sulfation in cell biology. Although most protein sulfation and sulfate demand occurs in cartilage synthesis, other cell constituents are also sulfated. Common sulfated substrates include cholesterol, steroid hormones, and sulfolipids (36). Cholesterol sulfate regulates the synthesis pathway of cholesterol (37), and heparan sulfate is a cofactor of several signaling receptors and growth factors (38, 39). Thus, the multiple structural and regulatory roles of sulfation are essential for all chondrocyte functions that mediate bone formation. This study suggests that the main chondrocyte sulfate supplier is Slc26a2, which provides SO_4^{2-} for both structural and regulatory proteins. This is likely unique to chondrocytes and osteoblasts (40) because other cells may not require Slc26a2 for signaling and development, as is suggested by a primarily skeletal phenotype in DTD. Because Slc26a2 is also expressed at high levels in the kidney, (Fig. 1), likely at the luminal membrane of proximal tubule (41), and in the colon (26), it should be of interest to determine the renal and intestinal phenotype of DTD.

Acknowledgments—We thank Dr. Daniella M. Schwartz for suggestions and editing of the manuscript.

REFERENCES

1. Mariani, F. V., and Martin, G. R. (2003) Deciphering skeletal patterning. Clues from the limb. *Nature* **423,** 319–325
2. DeLise, A. M., Fischer, L., and Tuan, R. S. (2000) Cellular interactions and signaling in cartilage development. *Osteoarthritis Cartilage* **8,** 309–334
3. de Andrea, C. E., and Hogendoorn, P. C. (2012) Epiphyseal growth plate and secondary peripheral chondrosarcoma. The neighbours matter. *J. Pathol.* **226,** 219–228
4. Häcker, U., Nybakken, K., and Perrimon, N. (2005) Heparan sulphate proteoglycans. The sweet side of development. *Nat. Rev. Mol. Cell Biol.* **6,** 530–541
5. Kronenberg, H. M. (2003) Developmental regulation of the growth plate. *Nature* **423,** 332–336
6. Danišovič, L., Varga, I., and Polák, S. (2012) Growth factors and chondrogenic differentiation of mesenchymal stem cells. *Tissue Cell* **44,** 69–73
7. Liu, J. P., Baker, J., Perkins, A. S., Robertson, E. J., and Efstratiadis, A. (1993) Mice carrying null mutations of the genes encoding insulin-like growth factor I (Igf-1) and type 1 IGF receptor (Igf1r). *Cell* **75,** 59–72
8. Zapf, J., and Froesch, E. R. (1986) Pathophysiological and clinical aspects of the insulin-like growth factors. *Horm. Res.* **24,** 160–165
9. Cooper, K. L., Oh, S., Sung, Y., Dasari, R. R., Kirschner, M. W., and Tabin, C. J. (2013) Multiple phases of chondrocyte enlargement underlie differences in skeletal proportions. *Nature* **495,** 375–378
10. Ohana, E., Shcheynikov, N., Park, M., and Muallem, S. (2012) Solute carrier family 26 member a2 (Slc26a2) protein functions as an electroneutral SOFormula/OH^-/Cl^- exchanger regulated by extracellular Cl. *J. Biol. Chem.* **287,** 5122–5132
11. Forlino, A., Piazza, R., Tiveron, C., Della Torre, S., Tatangelo, L., Bonafè, L., Gualeni, B., Romano, A., Pecora, F., Superti-Furga, A., Cetta, G., and Rossi, A. (2005) A diastrophic dysplasia sulfate transporter (SLC26A2) mutant mouse. Morphological and biochemical characterization of the resulting chondrodysplasia phenotype. *Hum. Mol. Genet.* **14,** 859–871
12. Superti-Furga, A., Rossi, A., Steinmann, B., and Gitzelmann, R. (1996) A chondrodysplasia family produced by mutations in the diastrophic dysplasia sulfate transporter gene. Genotype/phenotype correlations. *Am. J. Med. Genet.* **63,** 144–147
13. Gualeni, B., Facchini, M., De Leonardis, F., Tenni, R., Cetta, G., Viola, M., Passi, A., Superti-Furga, A., Forlino, A., and Rossi, A. (2010) Defective proteoglycan sulfation of the growth plate zones causes reduced chondrocyte proliferation via an altered Indian hedgehog signalling. *Matrix Biol.* **29,** 453–460
14. Mertz, E. L., Facchini, M., Pham, A. T., Gualeni, B., De Leonardis, F., Rossi, A., and Forlino, A. (2012) Matrix disruptions, growth, and degradation of cartilage with impaired sulfation. *J. Biol. Chem.* **287,** 22030–22042
15. Cornaglia, A. I., Casasco, A., Casasco, M., Riva, F., and Necchi, V. (2009) Dysplastic histogenesis of cartilage growth plate by alteration of sulphation pathway. A transgenic model. *Connect. Tissue Res.* **50,** 232–242
16. Zhang, X., Ziran, N., Goater, J. J., Schwarz, E. M., Puzas, J. E., Rosier, R. N., Zuscik, M., Drissi, H., and O'Keefe, R. J. (2004) Primary murine limb bud mesenchymal cells in long-term culture complete chondrocyte differentiation. TGF-β delays hypertrophy and PGE2 inhibits terminal differentiation. *Bone* **34,** 809–817
17. Park, S., Shcheynikov, N., Hong, J. H., Zheng, C., Suh, S. H., Kawaai, K., Ando, H., Mizutani, A., Abe, T., Kiyonari, H., Seki, G., Yule, D., Mikoshiba, K., and Muallem, S. (2013) Irbit mediates synergy between Ca^{2+} and cAMP signaling pathways during epithelial transport in mice. *Gastroenterology* **145,** 232–241
18. Rossi, A., Kaitila, I., Wilcox, W. R., Rimoin, D. L., Steinmann, B., Cetta, G., and Superti-Furga, A. (1998) Proteoglycan sulfation in cartilage and cell cultures from patients with sulfate transporter chondrodysplasias. Relationship to clinical severity and indications on the role of intracellular sulfate production. *Matrix Biol.* **17,** 361–369
19. Guérit, D., Philipot, D., Chuchana, P., Toupet, K., Brondello, J. M., Mathieu, M., Jorgensen, C., and Noël, D. (2013) Sox9-regulated miRNA-574-3p inhibits chondrogenic differentiation of mesenchymal stem cells. *PLoS ONE* **8,** e62582
20. Wong, M., Siegrist, M., and Goodwin, K. (2003) Cyclic tensile strain and

cyclic hydrostatic pressure differentially regulate expression of hypertrophic markers in primary chondrocytes. *Bone* **33,** 685–693
21. Patil, A. S., Sable, R. B., and Kothari, R. M. (2012) Role of insulin-like growth factors (IGFs), their receptors and genetic regulation in the chondrogenesis and growth of the mandibular condylar cartilage. *J. Cell. Physiol.* **227,** 1796–1804
22. Wang, Y., Nishida, S., Sakata, T., Elalieh, H. Z., Chang, W., Halloran, B. P., Doty, S. B., and Bikle, D. D. (2006) Insulin-like growth factor-I is essential for embryonic bone development. *Endocrinology* **147,** 4753–4761
23. Wang, F., Ijuin, T., Itoh, T., and Takenawa, T. (2011) Regulation of IGF-1/PI3K/Akt signalling by the phosphoinositide phosphatase pharbin. *J. Biochem.* **150,** 83–93
24. Starkman, B. G., Cravero, J. D., Delcarlo, M., and Loeser, R. F. (2005) IGF-I stimulation of proteoglycan synthesis by chondrocytes requires activation of the PI 3-kinase pathway but not ERK MAPK. *Biochem. J.* **389,** 723–729
25. Dwyer, E., Hyland, J., Modaff, P., and Pauli, R. M. (2010) Genotype-phenotype correlation in DTDST dysplasias: atelosteogenesis type II and diastrophic dysplasia variant in one family. *Am. J. Med. Genet.* **152,** 3043–3050
26. Haila, S., Hästbacka, J., Böhling, T., Karjalainen-Lindsberg, M. L., Kere, J., and Saarialho-Kere, U. (2001) SLC26A2 (diastrophic dysplasia sulfate transporter) is expressed in developing and mature cartilage but also in other tissues and cell types. *J. Histochem. Cytochem.* **49,** 973–982
27. Dorwart, M. R., Shcheynikov, N., Yang, D., and Muallem, S. (2008) The solute carrier 26 family of proteins in epithelial ion transport. *Physiology* **23,** 104–114
28. Markovich, D., and Aronson, P. S. (2007) Specificity and regulation of renal sulfate transporters. *Annu. Rev. Physiol.* **69,** 361–375
29. Beier, F., and Loeser, R. F. (2010) Biology and pathology of Rho GTPase, PI-3 kinase-Akt, and MAP kinase signaling pathways in chondrocytes. *J. Cell. Biochem.* **110,** 573–580
30. Mohan, S., and Kesavan, C. (2012) Role of insulin-like growth factor-1 in the regulation of skeletal growth. *Curr. Osteoporos. Rep.* **10,** 178–186
31. Accardi, A., and Miller, C. (2004) Secondary active transport mediated by a prokaryotic homologue of ClC Cl^- channels. *Nature* **427,** 803–807
32. Harrington, E. K., Coon, D. J., Kern, M. F., and Svoboda, K. K. (2010) PTH stimulated growth and decreased Col-X deposition are phosphotidylinositol-3,4,5 triphosphate kinase and mitogen activating protein kinase dependent in avian sterna. *Anat. Rec.* **293,** 225–234
33. Macrae, V. E., Ahmed, S. F., Mushtaq, T., and Farquharson, C. (2007) IGF-I signalling in bone growth. Inhibitory actions of dexamethasone and IL-1β. *Growth Horm. IGF Res.* **17,** 435–439
34. Ulici, V., Hoenselaar, K. D., Gillespie, J. R., and Beier, F. (2008) The PI3K pathway regulates endochondral bone growth through control of hypertrophic chondrocyte differentiation. *BMC Dev. Biol.* **8,** 40
35. Rokutanda, S., Fujita, T., Kanatani, N., Yoshida, C. A., Komori, H., Liu, W., Mizuno, A., and Komori, T. (2009) Akt regulates skeletal development through GSK3, mTOR, and FoxOs. *Dev. Biol.* **328,** 78–93
36. Diez-Roux, G., and Ballabio, A. (2005) Sulfatases and human disease. *Annu Rev. Genomics Hum. Genet.* **6,** 355–379
37. Strott, C. A., and Higashi, Y. (2003) Cholesterol sulfate in human physiology. What's it all about? *J. Lipid Res.* **44,** 1268–1278
38. Koziel, L., Kunath, M., Kelly, O. G., and Vortkamp, A. (2004) Ext1-dependent heparan sulfate regulates the range of Ihh signaling during endochondral ossification. *Dev. Cell* **6,** 801–813
39. Schönherr, E., and Hausser, H. J. (2000) Extracellular matrix and cytokines. A functional unit. *Dev. Immunol.* **7,** 89–101
40. Gualeni, B., de Vernejoul, M. C., Marty-Morieux, C., De Leonardis, F., Franchi, M., Monti, L., Forlino, A., Houillier, P., Rossi, A., and Geoffroy, V. (2013) Alteration of proteoglycan sulfation affects bone growth and remodeling. *Bone* **54,** 83–91
41. Chapman, J. M., and Karniski, L. P. (2010) Protein localization of SLC26A2 (DTDST) in rat kidney. *Histochem. Cell Biol.* **133,** 541–547